NASA Technical Memorandum 101355
ICOMP-88-18

# A Numerical Study of ENO and TVD Schemes for Shock Capturing



Shih-Hung Chang
*Cleveland State University*
*Cleveland, Ohio*

*and Institute for Computational Mechanics in Propulsion*
*Lewis Research Center*
*Cleveland, Ohio*

and

Meng-Sing Liou
*Lewis Research Center*
*Cleveland, Ohio*

September 1988

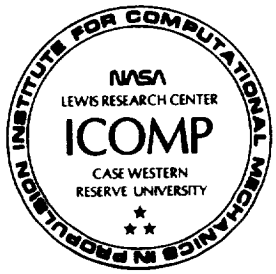


NASA

# A NUMERICAL STUDY OF ENO AND TVD SCHEMES FOR SHOCK CAPTURING

Shih-Hung Chang*
Department of Mathematics, Cleveland State University
Cleveland, Ohio 44115
and
Institute for Computational Mechanics in Propulsion (ICOMP)
Lewis Research Center
Cleveland, Ohio 44135

and

Meng-Sing Liou
National Aeronautics and Space Administration
Lewis Research Center
Cleveland, Ohio 44135

## SUMMARY

The numerical performance of a second-order upwind-based TVD scheme and that of a uniform second-order ENO scheme for shock capturing are compared. The TVD scheme used in this study is a modified version of Liou, using the flux-difference splitting (FDS) of Roe and his "superbee" function as the limiter. The construction of the basic ENO scheme is based on Harten, Engquist, Osher, and Chakravarthy, and the 2D extensions are obtained by using a Strang-type of fractional-step time-splitting method. Numerical results presented include both steady and unsteady, 1D and 2D calculations. All the chosen test problems have exact solutions so that numerical performance can be measured by comparing the computed results to them. For 1D calculations, the standard shock-tube problems of Sod and Lax are chosen. A very strong shock-tube problem, with the initial density ratio of 400 to 1 and pressure ratio of 500 to 1, is also used to study the behavior of the two schemes. For 2D calculations, the shock wave reflection problems are adopted for testing. The cases presented in this report include flows with Mach numbers of 2.9, 5.0, and 10.0.

*Work funded under Space Act Agreement C99066G.

## INTRODUCTION

For hyperbolic systems of conservation laws, conventional shock capturing schemes are known to yield oscillatory solutions near discontinuities. The requirement of monotonicity has led to the notion of the total variation diminishing[1] (TVD) property that provides a mathematical basis for the subsequent development of many TVD schemes. One large class of TVD schemes uses flux limiters to control the amount of anti-diffusive flux[1-7]. The limiter can be designed so that a conventional non-TVD scheme may be modified to satisfy the TVD condition[1]. Formal extensions of these ideas have also been made to a variety of problems in multidimensions[8,9].

Although "high-order" TVD schemes generally show oscillation-free and crisp shock profiles, they degenerate to first-order accuracy at extremum points of the solution. Also, it was shown that TVD schemes are at most first-order accurate in multidimensions[10]. Partly aimed at removing the local restrictions of the TVD schemes, Harten, Engquist, Osher, and Chakravarthy recently developed the uniformly accurate essentially non-oscillatory (ENO) scheme[11,12]. Instead of restricting the total variation from increasing as in TVD, the ENO scheme permits the variation to possibly increase, but only by an amount on the level of local truncation errors.

The basic ENO-theory contains many desirable properties. The essential feature that distinguishes the ENO construction from other shock capturing schemes is the use of piecewise polynomials to obtain an essentially non-oscillatory reconstruction of the solution from its cell averages. Because the ENO scheme is relatively new, its numerical performance has yet to be fully explored. A numerical comparison of the ENO and the TVD schemes based on Chakravarthy and Osher[13] is contained in Chakravarthy et al[14], where the numerical experiment was done on a linear scalar equation showing the superiority of the ENO over TVD, which clips at the local extremum of the smooth solution. Although clearly the ENO scheme is applicable to the approximation of any solution, smooth or discontinuous, it seems that the main purpose of its development is still to capture shocks. One would like to study further the behavior of the ENO as a shock capturing scheme. One of the major tasks is to investigate whether this new approach can be extended to produce higher-order multidimensional shock capturing schemes.

In practical applications a uniform second-order scheme is very desirable. In this report, we investigate the numerical performance of a second-order upwind-based TVD scheme and that of a uniform second-order ENO scheme for shock capturing. We understand that not all TVD schemes perform equally well due to the differences in construction. The TVD scheme used in this study is a modified version of Liou[7], using Roe's flux-difference splitting (FDS)[15] and his "superbee" function[5] as the limiter. The construction of the basic ENO scheme is based on Harten et al[11] and the 2D extensions presented here are obtained by using a Strang-type of fractional-step time-splitting method[16]. Results presented in the following sections include both steady and unsteady, 1D and 2D calculations. For 1D calculations, we use the standard shock-tube test problems of Sod and Lax. A very strong shock-tube problem, with the initial density ratio of 400 to 1 and pressure ratio of 500 to 1, is also used to study the

behavior of the two schemes. For 2D calculations, we adopt the shock wave reflection problems for testing so that numerical results can be compared with the exact solutions. The cases presented here include flows with Mach numbers of 2.9, 5.0, and 10.0.

## CONSTRUCTION OF THE SCHEMES

In this section we describe briefly the construction of both schemes.

ENO Scheme:

Rather than repeating Ref.11, we describe in the following a step-by-step algorithm for implementing a uniform second-order ENO scheme using the reconstruction via deconvolution (RD).

For a single conservation law of the form

$$u_t + f(u)_x = 0, \qquad t > 0, \tag{1}$$

$$u(x,0) = u_0(x), \tag{2}$$

the integration of (1) over $[x_{i-\frac{1}{2}}, x_{i+\frac{1}{2}}]\times[t_n, t_{n+1}]$ leads to

$$\overline{u}_i^{n+1} = \overline{u}_i^n - \frac{\Delta t}{\Delta x}(\hat{f}_{i+\frac{1}{2}} - \hat{f}_{i-\frac{1}{2}}), \tag{3}$$

where

$$\hat{f}_{i+\frac{1}{2}} = \frac{1}{\Delta t}\int_0^{\Delta t} f(u(x_{i+\frac{1}{2}}, t_n + \mu))d\mu, \tag{4}$$

and $\overline{u}_i^n$ denotes the cell-average of $u$ over $[x_{i-\frac{1}{2}}, x_{i+\frac{1}{2}}]$ at $t_n$. In this formulation, one sees that the function $u$ in the integral in (4) has to be reconstructed from the cell-averages $\{\overline{u}_i^n\}$. The ENO scheme uses piecewise polynomials to obtain an essentially non-oscillatory reconstruction $u(x,t_n)$, and then uses a local Taylor expansion to obtain $u(x,t)$ over $[t_n, t_{n+1}]$.

At $t_n$, assume that we have obtained $\{v_i^n\}$ approximating $\{\overline{u}_i^n\}$. The $\{v_i^n\}$ comes from the numerical scheme

$$v_i^{n+1} = v_i^n - \frac{\Delta t}{\Delta x}(\overline{f}_{i+\frac{1}{2}} - \overline{f}_{i-\frac{1}{2}}), \tag{5}$$

where

$$\overline{f}_{i+\frac{1}{2}} = \frac{1}{\Delta t}\int_0^{\Delta t} f(v(x_{i+\frac{1}{2}}, t_n + \mu))d\mu. \tag{6}$$

In order to compute $\overline{f}_{i+\frac{1}{2}}$ in (6), we first reconstruct $v$ from $\{v_i^n\}$. For a second-order scheme, the reconstructed $v$ at $t_n$ takes the form

$$v(x,t_n) = v_i^n + s_i(x - x_i), \quad \text{over each } [x_{i-\frac{1}{2}}, x_{i+\frac{1}{2}}], \tag{7}$$

where the slope $s_i$ is chosen in the following way.

For each $[x_i, x_{i+1}]$, if

$$|v_{i+1}^n - 2v_i^n + v_{i-1}^n| < |v_{i+2}^n - 2v_{i+1}^n + v_i^n|,$$

set

$$\frac{d}{dx}v(x_i + 0) = \frac{1}{2\Delta x}(v_{i+1}^n - v_{i-1}^n),$$
$$\frac{d}{dx}v(x_{i+1} - 0) = \frac{1}{2\Delta x}(3v_{i+1}^n - 4v_i^n + v_{i-1}^n);$$

else set

$$\frac{d}{dx}v(x_i + 0) = \frac{1}{2\Delta x}(-v_{i+2}^n + 4v_{i+1}^n - 3v_i^n),$$
$$\frac{d}{dx}v(x_{i+1} - 0) = \frac{1}{2\Delta x}(v_{i+2}^n - v_i^n),$$

where $\frac{d}{dx}v(x_i + 0)$ and $\frac{d}{dx}v(x_i - 0)$ denote one-sided derivatives at $x_i$ from the right and the left respectively. Then

$$s_i = M\big(\frac{d}{dx}v(x_i - 0), \frac{d}{dx}v(x_i + 0)\big), \tag{8}$$

where $M$ denotes the minmod function

$$M(p, q) = \begin{cases} \sigma\ min(|p|, |q|), & \text{if } Sgn(p) = Sgn(q) = \sigma; \\ 0, & \text{otherwise.} \end{cases}$$

The above algebraic procedure for the reconstruction of $v$ is illustrated in Fig. 1. In the picture shown, we have $|v_{i+1}^n - 2v_i^n + v_{i-1}^n| < |v_{i+2}^n - 2v_{i+1}^n + v_i^n|$. Then we construct a quadratic polynomial passing through $v_{i-1}$, $v_i$, and $v_{i+1}$. The slopes of the two one-sided tangents to this polynomial at $x_i$ and $x_{i+1}$ are denoted by $\frac{d}{dx}v(x_i + 0)$ and $\frac{d}{dx}v(x_{i+1} - 0)$ respectively. Hence, doing this construction over every $[x_i, x_{i+1}]$, we will get two one-sided slopes at every point $v_i$. The minmod function $M$ is then used to select the final slope.

Next, we construct the local Taylor expansion $\tilde{v}_i(x, t)$ over $[x_{i-\frac{1}{2}}, x_{i+\frac{1}{2}}] \times [t_n, t_{n+1}]$ using the original PDE (1) and $\tilde{v}_i(x, t_n) = v(x, t_n)$ as the initial values. For a second-order scheme, we truncate the second and higher-order terms in the Taylor expansion.

Now, it is also sufficient for a second-order scheme to approximate the integral in (6) by using the trapezoidal rule. We obtain

$$\overline{f}_{i+\frac{1}{2}} = \frac{1}{2}\big[f(v(x_{i+\frac{1}{2}}, t_n)) + f(v(x_{i+\frac{1}{2}}, t_{n+1}))\big]. \tag{9}$$

Here in (9) each $f(v(x_{i+\frac{1}{2}}, t))$ is then approximated by

$$f^R(\tilde{v}_i(x_{i+\frac{1}{2}}, t), \tilde{v}_{i+1}(x_{i+\frac{1}{2}}, t)),$$

where $f^R(v_L, v_R) = f(V(0; v_L, v_R))$ and $V(x/t; v_L, v_R)$ denotes the self-similar solution to the Riemann problem

$$v_t + f(v)_x = 0, \qquad t > 0,$$
$$v(x,0) = \begin{cases} v_L, & x < 0, \\ v_R, & x > 0. \end{cases}$$

Note that a Riemann solver can be adopted here to obtain the values $f^R$.

Hence, combining the above we have

$$v_i^{n+1} = v_i^n - \frac{\Delta t}{\Delta x}(\overline{f}_{i+\frac{1}{2}} - \overline{f}_{i-\frac{1}{2}}), \tag{10}$$

where

$$\overline{f}_{i+\frac{1}{2}} = \frac{1}{2}\big[f^R(\tilde{v}_i(x_{i+\frac{1}{2}}, t_n), \tilde{v}_{i+1}(x_{i+\frac{1}{2}}, t_n)) + f^R(\tilde{v}_i(x_{i+\frac{1}{2}}, t_{n+1}), \tilde{v}_{i+1}(x_{i+\frac{1}{2}}, t_{n+1}))\big], \tag{11}$$

with

$$\tilde{v}_i(x_{i+\frac{1}{2}}, t_n) = v_i^n + \frac{\Delta x}{2} s_i,$$
$$\tilde{v}_{i+1}(x_{i+\frac{1}{2}}, t_n) = v_{i+1}^n - \frac{\Delta x}{2} s_{i+1},$$
$$\tilde{v}_i(x_{i+\frac{1}{2}}, t_{n+1}) = v_i^n + \frac{\Delta x}{2} s_i - \Delta t f'(v_i^n) s_i,$$
$$\tilde{v}_{i+1}(x_{i+\frac{1}{2}}, t_{n+1}) = v_{i+1}^n - \frac{\Delta x}{2} s_{i+1} - \Delta t f'(v_{i+1}^n) s_{i+1},$$

and the $s_i$'s come from (8). This scheme is uniformly second-order accurate in the pointwise sense.

For a nonlinear system of conservation laws of the form

$$u_t + f(u)_x = 0, \qquad t > 0, \tag{12}$$
$$u(x,0) = u_0(x), \tag{13}$$

where $u(x,t) = (u_1(x,t), ..., u_m(x,t))^T$ and $f = (f_1, ..., f_m)^T$, we describe briefly the procedure using the characteristic reconstruction[11]. Let $a_i(u)$, i=1,...,m, denote the eigenvalues of the Jacobian matrix

$$A(u) = \frac{\partial f}{\partial u}$$

so that $a_1(u) \leq \cdots \leq a_m(u)$. Let $r_1(u), ..., r_m(u)$ be the corresponding linearly independent right-eigenvectors. Also, let $l_1(u), ..., l_m(u)$ denote the left-eigenvectors of $A(u)$ so that $l_i(u) r_k(u) = \delta_{ik}$. The $k^{th}$ characteristic variable is defined to be

$$w^k = l_k u, \qquad k = 1, ..., m.$$

Now, suppose we know the approximations $\{v_i^n\}$ to the cell-averages $\{\overline{u}(x_i,t_n)\}$, where $\overline{u}(x_i,t_n) = (\overline{u}_1(x_i,t_n),...,\overline{u}_m(x_i,t_n))^T$. For each fixed $i$ and a fixed $k$, we use the following values

$$l_k(v_i^n)v_{i-1}^n,...,l_k(v_i^n)v_{i+2}^n$$

and the procedure described in (7), (8) to reconstruct $w^k$ over $[x_{i-\frac{1}{2}},x_{i+\frac{1}{2}}]$ at $t_n$. Let $w^k(x,t_n)$ denote this reconstructed polynomial over $[x_{i-\frac{1}{2}},x_{i+\frac{1}{2}}]$. Then the vector-valued characteristic reconstruction $v(x,t_n)$ will be of the form

$$v(x,t_n) = \sum_{k=1}^{m} w^k(x,t_n)r_k(v_i^n), \quad \text{over } [x_{i-\frac{1}{2}},x_{i+\frac{1}{2}}].$$

Then we construct the local Taylor expansion $\tilde{v}_i(x,t)$ over $[x_{i-\frac{1}{2}},x_{i+\frac{1}{2}}]\times[t_n,t_{n+1}]$ using the original PDE (12) and $\tilde{v}_i(x,t_n) = v(x,t_n)$ as the initial values.

The resulting scheme for the system (12) will take the same form as (10) and (11), interpreted as vector equations. The values for $f^R$ are similarly obtained from a Riemann solver. For the Euler equations, one can use either an approximate Riemann solver (e.g. the one developed by Roe[15]) or an exact Riemann solver. The results presented here are obtained by using an exact Riemann solver outlined in Chorin[17].

For 2D computations, we present the results obtained by using the Strang-type of fractional-step time-splitting method[16]. The final 2D scheme is formally of second-order. Since this method has been well-documented in the literature (see, e.g., Ref. 8,17), we omit the details.

Upwind-Based TVD Scheme:

The construction of the upwind-based TVD schemes consists of basically the following steps:

(1) Decomposition by upwinding: The conventional representation of spatial flux derivatives, such as second- or higher-order, central or upwind difference, is decomposed into parts consisting of a first-order upwind flux difference and the remaining higher-order flux differences, called anti-diffusive terms. For example, one can choose the following second-order central difference formula

$$f(u)_x = \frac{1}{2\Delta x}(f_{i+1} - f_{i-1})$$

and decompose it into a first-order upwinding term plus an anti-diffusive term as follows

$$f_x = \frac{1}{\Delta x}(\Delta^+ f^- + \Delta^- f^+) + \frac{1}{2\Delta x}\Delta^-(\Delta^+ f^+ - \Delta^+ f^-),$$

where $\Delta^+$ and $\Delta^-$ denote the forward and backward differences, $f^+$ and $f^-$ denote the positive and negative fluxes.

(2) Recombination by limiters: Introduce flux-difference limiters, $\phi^+$ and $\phi^-$, to the anti-diffusive terms,

$$f_x = \frac{1}{\Delta x}(\Delta^+ f^- + \Delta^- f^+) + \frac{1}{2\Delta x}\Delta^-(\phi^+\Delta^+ f^+ - \phi^-\Delta^+ f^-).$$

(3) Time evolution by TVD: Choose a time integration scheme, e.g., the Lax-Wendroff or the two-stage Runge-Kutta scheme as used in the present study, and determine the functional form of limiters for satisfying the TVD condition[1]. The results presented here are obtained by using Roe's "superbee" function[5] as the limiters.

Hence the critical ingredients are the upwinding and the choice of limiters. In the scalar case, there are no essential variations in defining the argument of the limiter function among TVD schemes; the variations are wider in the case of systems of equations.

In Ref.7, the upwinding procedure is achieved by the flux-vector splittings (FVS) of Steger and Warming[18], and van Leer[19]. Since the construction of the present TVD scheme is done in terms of flux differences representing the spatial derivatives, as shown above, the flux-difference splittings (FDS) of Roe[15] and Osher[20] become a natural vehicle for upwinding. In fact, replacing the subroutine evaluating the FVS by that for FDS was the only change needed in the code.

The procedure developed for the scalar hyperbolic equation is generalized to the one-dimensional system of conservation laws, which can be decoupled into scalar equations for each of the characteristic variables in the constant coefficient case. For more details on the TVD construction and various forms of the limiter functions for the system, see Ref.7. A formal extension to multidimensional equations is made by treating the flux derivative in each direction individually, following the spirit of the directional splitting as stated earlier in the construction of the ENO scheme. This treatment, while straightforward in implementation, will result in a wider smearing at a discontinuity in multidimension.

## NUMERICAL TESTS AND COMPARISON

We have chosen test problems with known exact solutions to make meaningful comparisons. For 1D calculations, we show the numerical results for three unsteady shock tube problems with shock strengths ranging from moderate to very strong. Here 1D Euler equations are solved in both schemes. TVD calculations are carried out using the flux-difference splitting (FDS) [15] and the "superbee" function[5] as the limiter. In Fig. 2, 3, and 4, we show both the computed and the exact solutions after certain time steps. For comparison in each figure, the TVD results are shown in the (a)-sets of figures and the ENO results in the (b)-sets. The initial conditions are also plotted and they are given as follows.

Fig.2. Sod's Problem:

$$(\rho, u, p) = \begin{cases} (1, 0, 1), & x < 5 \\ (0.125, 0, 0.1), & x > 5. \end{cases}$$

Fig.3. Lax's Problem:

$$(\rho, u, p) = \begin{cases} (0.445, 0.698, 3.528), & x < 5 \\ (0.5, 0, 0.571), & x > 5. \end{cases}$$

Fig.4. Strong Shock Problem:

$$(\rho, u, p) = \begin{cases} (400, 0, 500), & x < 5 \\ (1, 0, 1), & x > 5. \end{cases}$$

For the Sod problem, we take $\Delta x = 0.1$, $\Delta t = 0.03$, and compare the results after 60 time-steps. Similarly, for the Lax problem, we take $\Delta x = 0.1$, $\Delta t = 0.017$, and 85 time-steps; and for the strong shock problem $\Delta x = 0.05$, $\Delta t = 0.01$, and 90 time-steps.

For 1D computations, the Sod and Lax problems involve only moderate strength shocks. Here both the TVD and ENO schemes show very good results. However, in comparison with the exact solutions, the TVD results appear to be slightly less dissipative than the ENO in describing both the shock and contact discontinuities, but less accurate in the head of the expansion fan. The shock strength in the third test problem is considerably higher than the first two cases, thereby presenting a more severe test on the schemes. Here, the ENO results seem to be better than the TVD results, although both schemes badly diffuse the contact discontinuity. In Fig.4, the severe rounding of energy-distributions is probably caused by the starting errors in the Riemann problem. In Fig.4(a), the "kink" in the velocity-distribution is caused by the flux-differencing in the scheme we used, but can be removed by adding a smoothing term. TVD schemes based on initial-value reconstruction such as van Leer's MUSCL, in general, do not have this phenomenon.

For multidimensional computations, in general, the shock capturing numerical schemes are formal extensions of the corresponding 1D schemes. In our case, both the TVD and ENO schemes are formally extended to 2D problems. We test the extended schemes on problems involving a regular reflection of an oblique shock wave from a plane wall. Here the 2D Euler equations are solved, with incoming Mach numbers ranging from 2.9 to 10.0 and a shock angle of 29 degrees. The physical situation is shown in Fig. 5. The TVD scheme is formally applied directly to the steady Euler equations, while the ENO scheme is formally applied via the Strang-type fractional steps to the unsteady Euler equations until steady solutions are reached. The inflow and the interior initial conditions are fully specified with free stream values, and the conditions at the top boundary are set to satisfy the shock-jump relations with a specified shock angle. The variables at the outflow boundary are extrapolated. At the solid wall, the vertical velocity component and the gradient of the other variables are set to zero. The computational domains contain equally divided meshes with $\Delta x = 0.067$ and $\Delta y = 0.05$. For the test cases with Mach numbers of 2.9, 5.0, and 10.0, the computational domains contain respectively 61x21, 74x21, and 83x21 points.

In the ENO computations, the case with Mach number 2.9 is straightforward. In the cases with Mach numbers 5.0 and 10.0, we have to degrade the scheme to the first-order Godunov scheme near very strong shocks. The reason for doing this is that the application of the same algorithm used in the Mach 2.9 case does not produce steady solutions for the higher Mach number cases. What happened was that, after the shocks were correctly captured, the computed solution would continue to change and convergence could not be reached. Our experiments indicate that the difficulty occurs when the Mach number reaches 4.0. We understand that in Glaz, Colella, Glass

and Deschambault[21] on a different numerical experiment, a similar reduction of order was made to their second-order Godunov scheme in the immediate vicinity of a strong shock.

In our 2D computations, although the results from both extended schemes are quite acceptable, they are not as crisp as those 1D results. In Fig. 6, we show the pressure contours of the Mach 2.9 ENO computation. A similar picture is obtained from the TVD computation. Since it is impossible to compare the accuracy of the results using these contour pictures, we look at the pressure distributions at the cross sections at $y = 0$ and $y = 0.5$. In Fig. 7, 8, and 9, we show both the computed and the exact steady solutions for the cases with Mach numbers of 2.9, 5.0, and 10.0 respectively. In comparison with the exact solution in the Mach 2.9 case, both the TVD and ENO results are quite good. ENO captures discontinuities using slightly fewer mesh points, but TVD is slightly less oscillatory here. For the cases with Mach numbers 5.0 and 10.0, our extended ENO results are inferior to the corresponding TVD results. This is due to the reduction to the first-order Godunov scheme near very strong shocks. Further investigation is undertaken to improve the method of implementation.

## ACKNOWLEDGMENTS

The authors would like to thank Bram van Leer for many helpful discussions and suggestions.

## REFERENCES

1. Harten, A., "High Resolution Schemes for Hyperbolic Conservation Laws," J. Comp. Phys., 49(1983), pp.357-393.
2. Van Leer, B., "Towards the Ultimate Conservative Difference Scheme II. Monotonicity and Conservation Combined in a Second-Order Scheme," J. Comp. Phys., 14(1974), pp. 361-370.
3. Osher, S. and Chakravarthy, S., "High Resolution Schemes and The Entropy Condition," SIAM J. Numer. Anal., 21(1984), pp. 955-984.
4. Sweby, P.K., "High Resolution Schemes Using Flux Limiters for Hyperbolic Conservation Laws," SIAM J. Numer. Anal., 21(1984), pp. 995-1011.
5. Roe, P.L., "Some Contributions to The Modelling of Discontinuous Flows," Lectures in Appl. Math., 22(1985), Part II, pp. 163-193.
6. Yee, H.C., Warming, R.F., and Harten, A., "Implicit Total Variation Diminishing(TVD) Schemes for Steady-State Calculations," J. Comp. Phys., 57(1985), pp. 327-360.
7. Liou, M.-S., "A Generalized Procedure for Constructing an Upwind-Based TVD Scheme," AIAA Paper 87-0355.
8. Yee, H. C., "Upwind and Symmetric Shock-Capturing Schemes," NASA TM89464, May 1987.

9. Yee, H.C., Klopfer, G.H., and Montagné, J.-L., "High-Resolution Shock-Capturing Schemes for Inviscid and Viscous Hypersonic Flows," NASA TM100097, April 1988.
10. Goodman, J.B. and LeVeque, R.J., "On the Accuracy of Stable Schemes for 2D Scalar Conservation Laws," Math. Comp., 45(1985), pp. 15-21.
11. Harten, A., Engquist, B., Osher, S., and Chakravarthy, S., "Uniformly High Order Accurate Essentially Non-Oscillatory Schemes III," J. Comp. Phys., 71(1987), pp. 231-303.
12. Harten, A. and Osher, S., "Uniformly High-Order Accurate Nonoscillatory Schemes I," SIAM J. Numer. Anal., 24(1987), pp. 279-309.
13. Chakravarthy, S.R. and Osher, S., "A New Class of High Accuracy TVD Schemes for Hyperbolic Conservation Laws," AIAA Paper 85-0363.
14. Chakravarthy, S.R., Harten, A., and Osher, S., "Essentially Non-Oscillatory Shock-Capturing Schemes of Arbitrarily-High Accuracy," AIAA Paper 86-0339.
15. Roe, P.L., "Approximate Riemann Solvers, Parameter Vectors, and Difference Schemes," J. Comp. Phys., 43(1981), pp. 357-372.
16. Strang, G., "On the Construction and Comparison of Difference Schemes," SIAM J. Numer. Anal., 5(1968), pp. 506-517.
17. Chorin, A.J., "Random Choice Solution of Hyperbolic Systems," J. Comp. Phys., 22(1976), pp. 517-533.
18. Steger, J.L. and Warming, R.F., "Flux Vector Splitting of the Inviscid Gasdynamic Equations with Application to Finite Difference Methods," J. Comp. Phys., 40(1981), pp. 263-293.
19. Van Leer, B., "Flux-Vector Splitting for the Euler Equations," Lecture Notes in Phys., 170(1982), pp. 507-512.
20. Osher, S., "Numerical Solution of Singular Perturbation Problems and Hyperbolic Systems of Conservation Laws," North-Holland Mathematical Studies, 47(1981), pp. 179-205.
21. Glaz, H.M., Colella, P., Glass, I.I. and Deschambault, R.L., "A Numerical Study of Oblique Shock-Wave Reflections with Experimental Comparisons," Proc. R. Soc. Lond. A 398(1985), pp. 117-140.

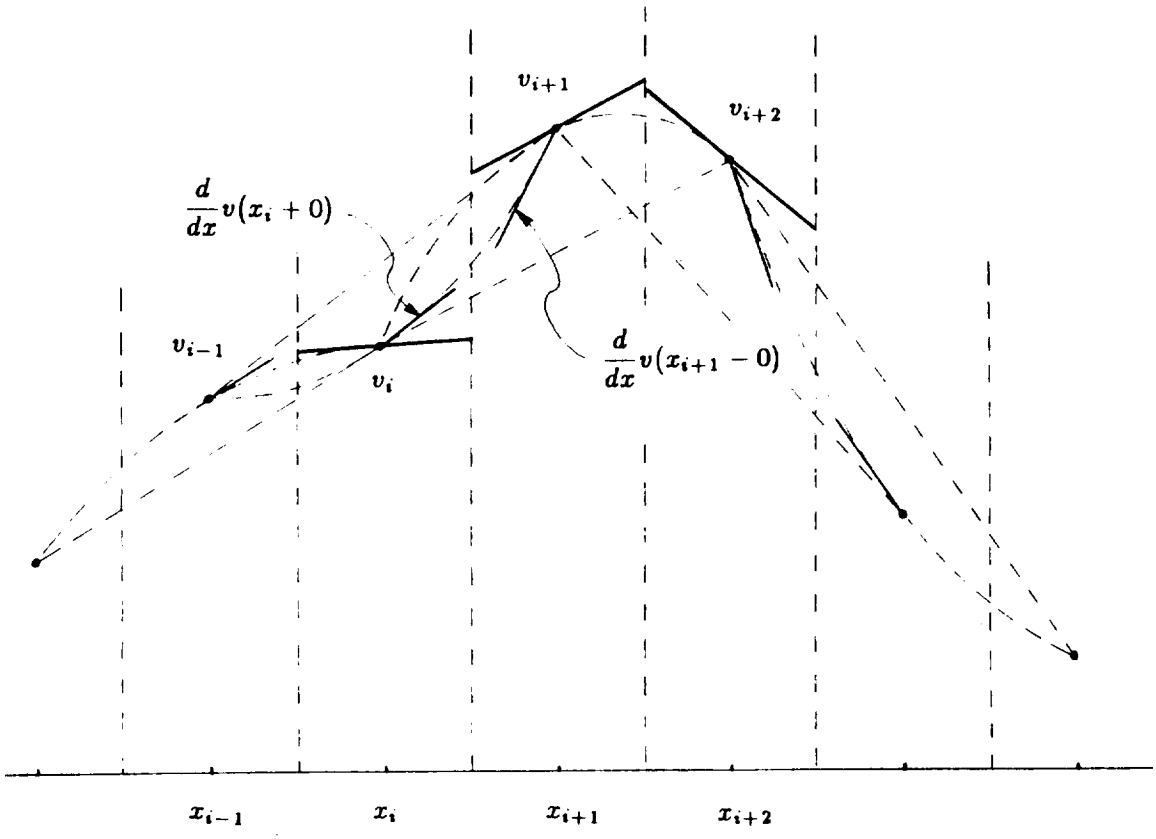


Fig. 1. Geometric ENO reconstruction

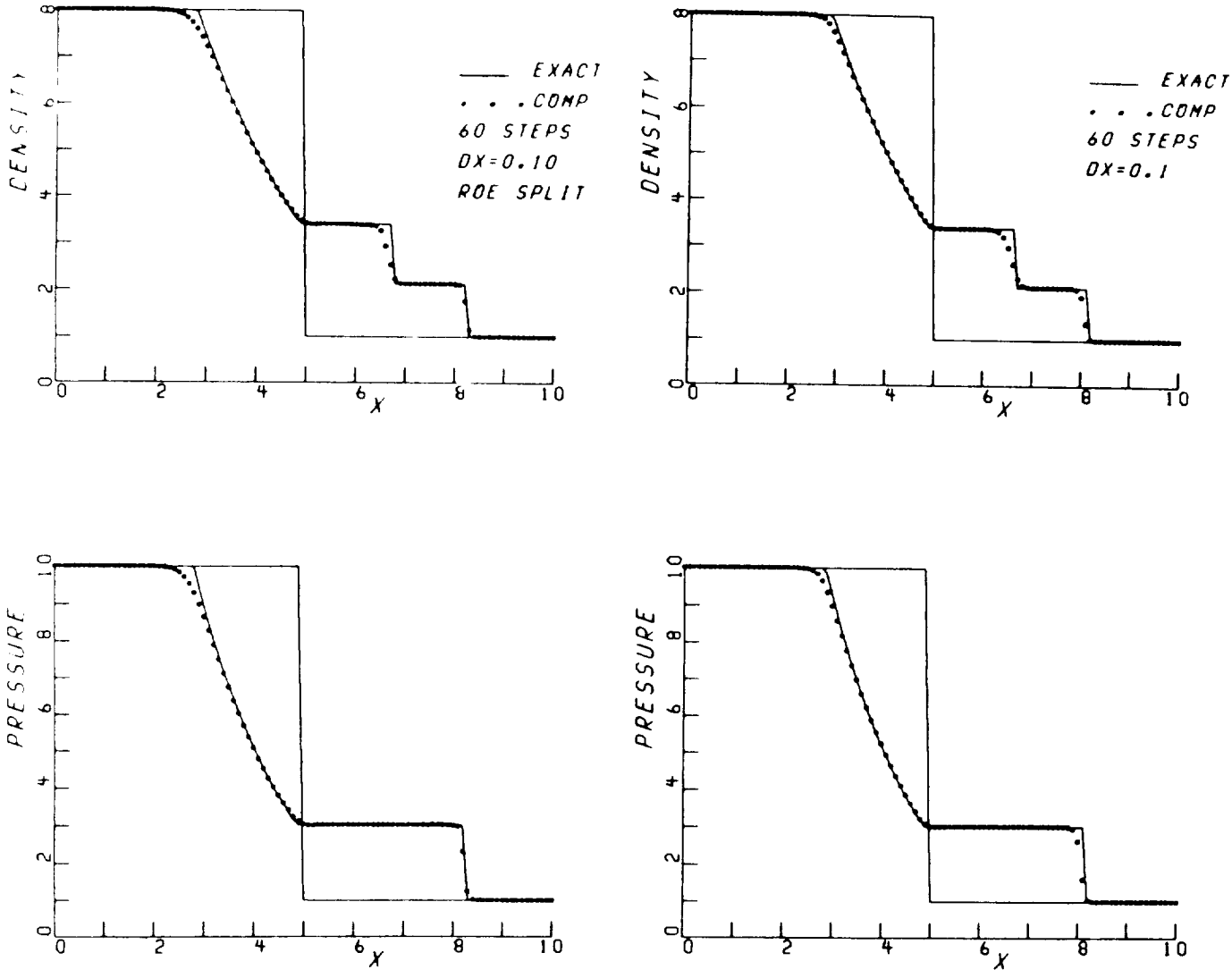


(a) TVD (b) ENO

Fig. 2. Numerical solutions of Sod's problem

$$(\rho, u, p) = \begin{cases} (1, 0, 1), & x < 5 \\ (0.125, 0, 0.1), & x > 5 \end{cases}$$

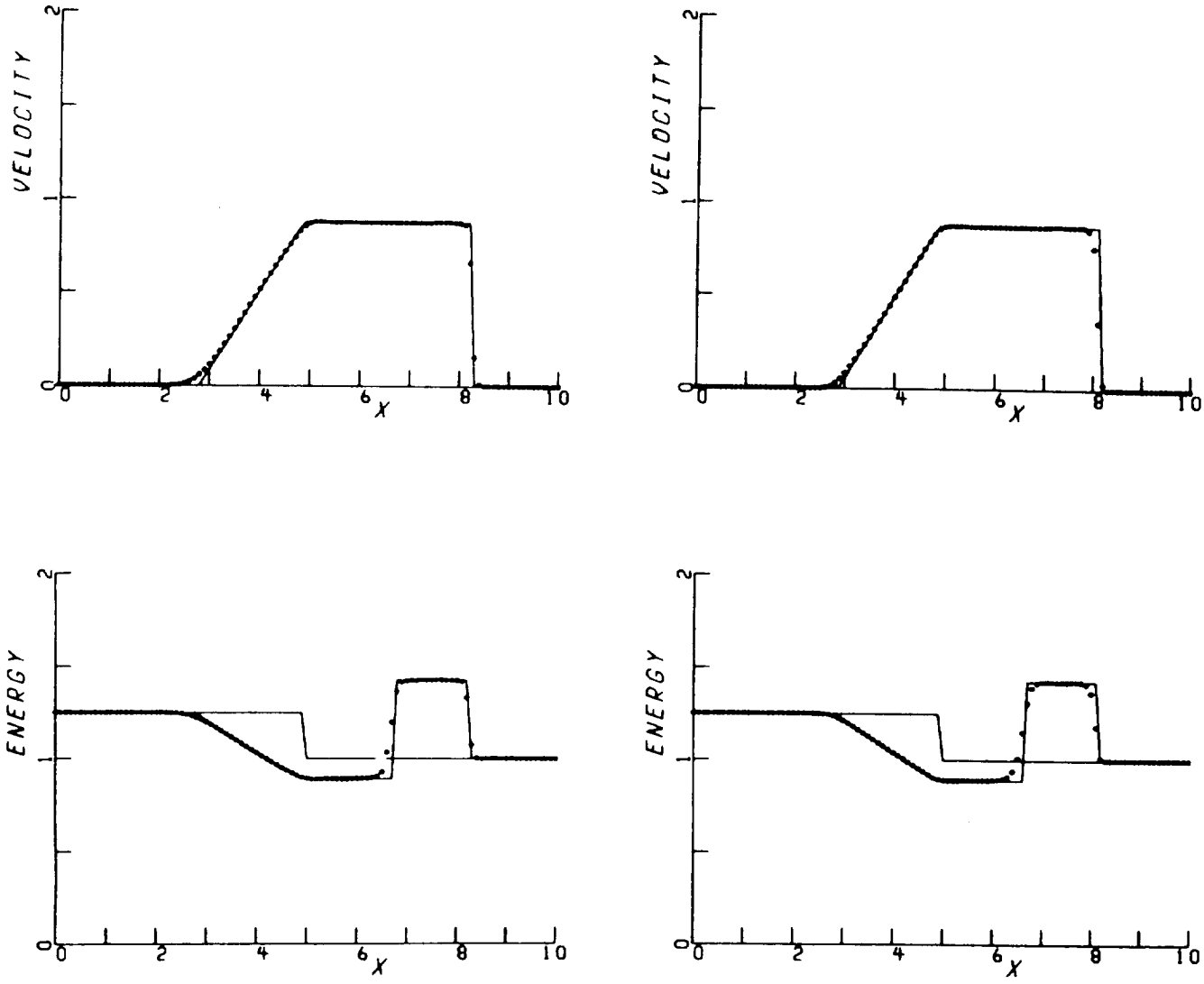


(a) TVD (b) ENO

Fig. 2. Numerical solutions of Sod's problem(continued)

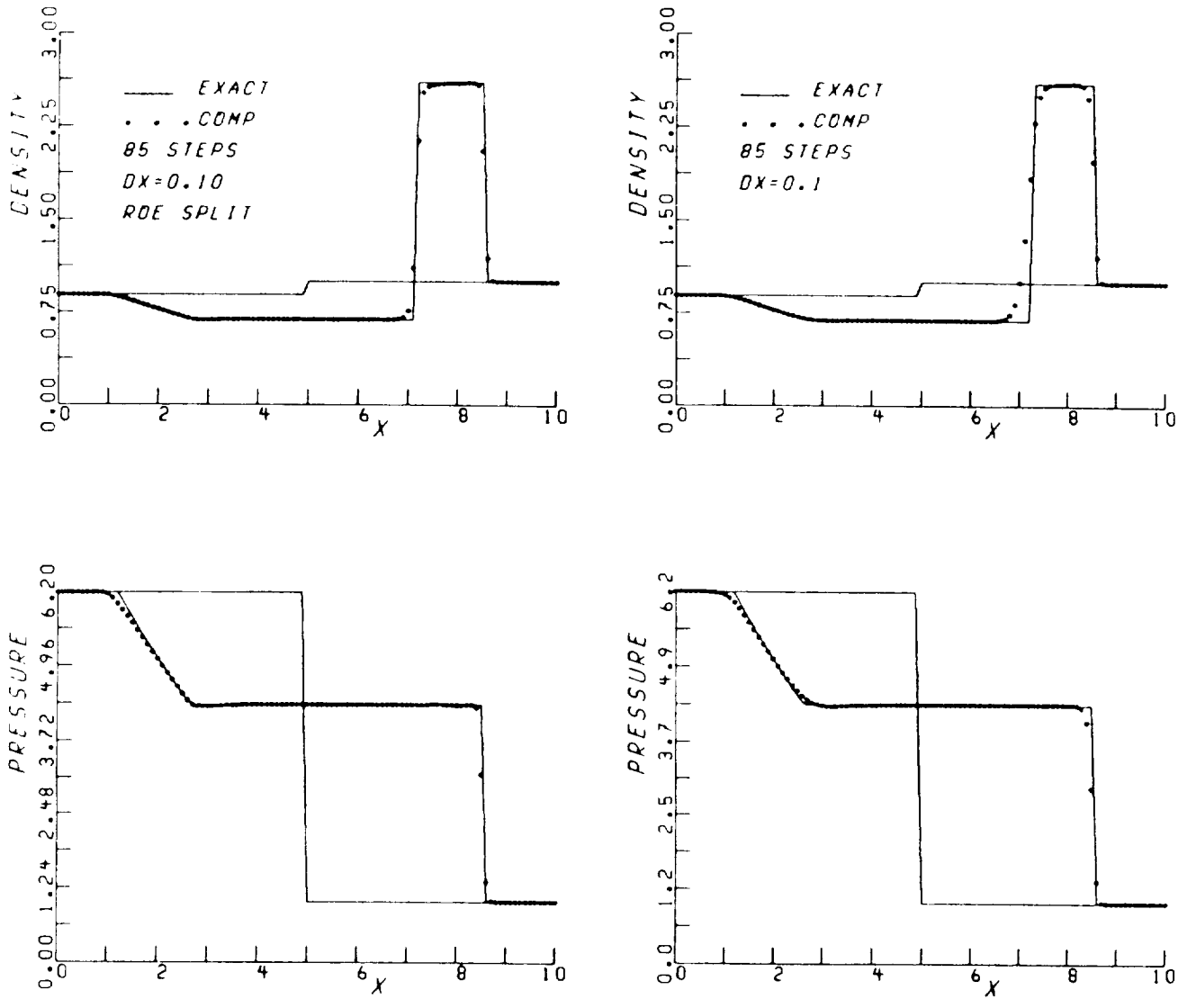


(a) TVD

(b) ENO

Fig. 3. Numerical solutions of Lax's problem

$$(\rho, u, p) = \begin{cases} (0.445, 0.698, 3.528), & x < 5 \\ (0.5, 0, 0.571), & x > 5 \end{cases}$$

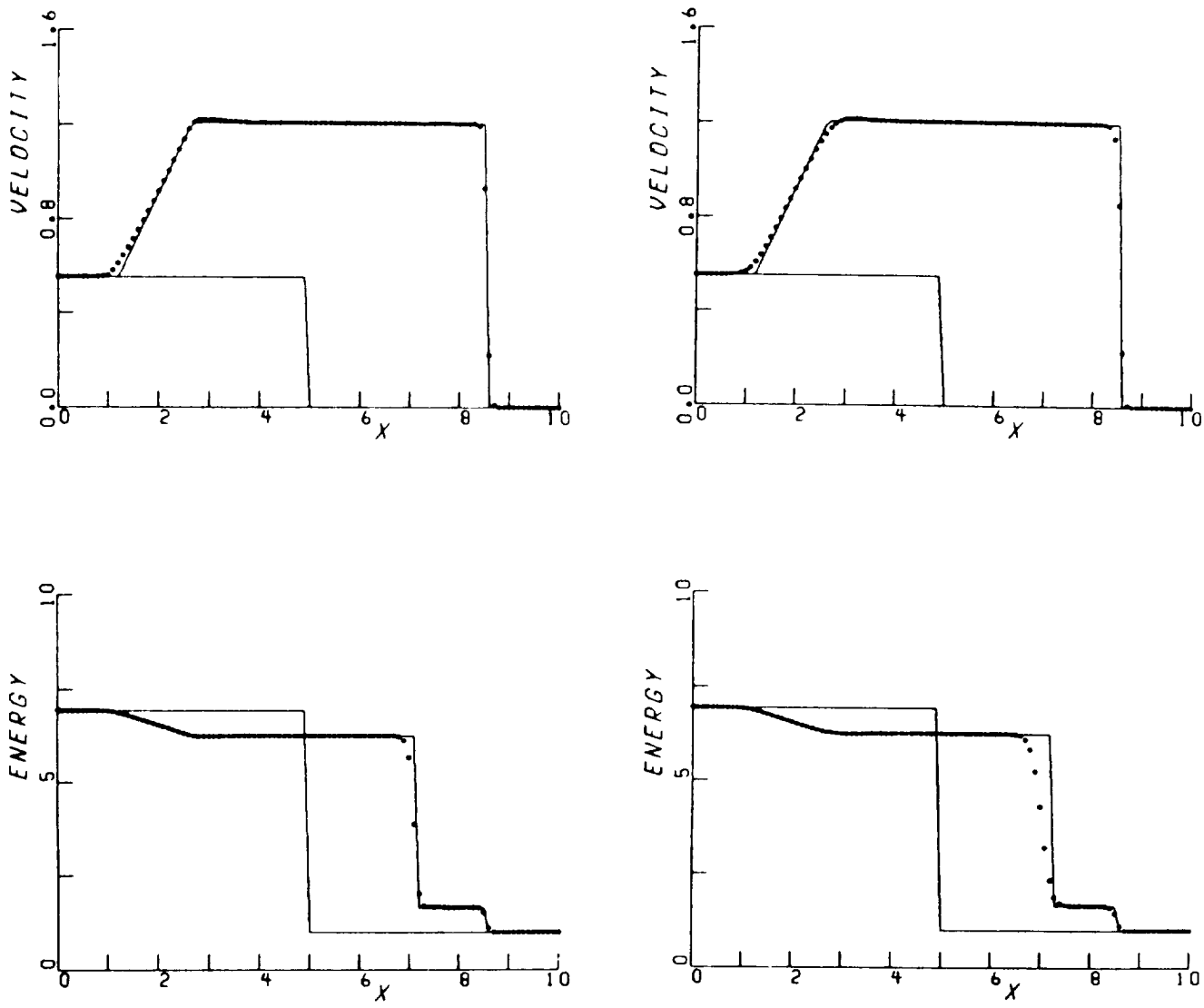


(a) TVD

(b) ENO

Fig. 3. Numerical solutions of Lax's problem(continued)

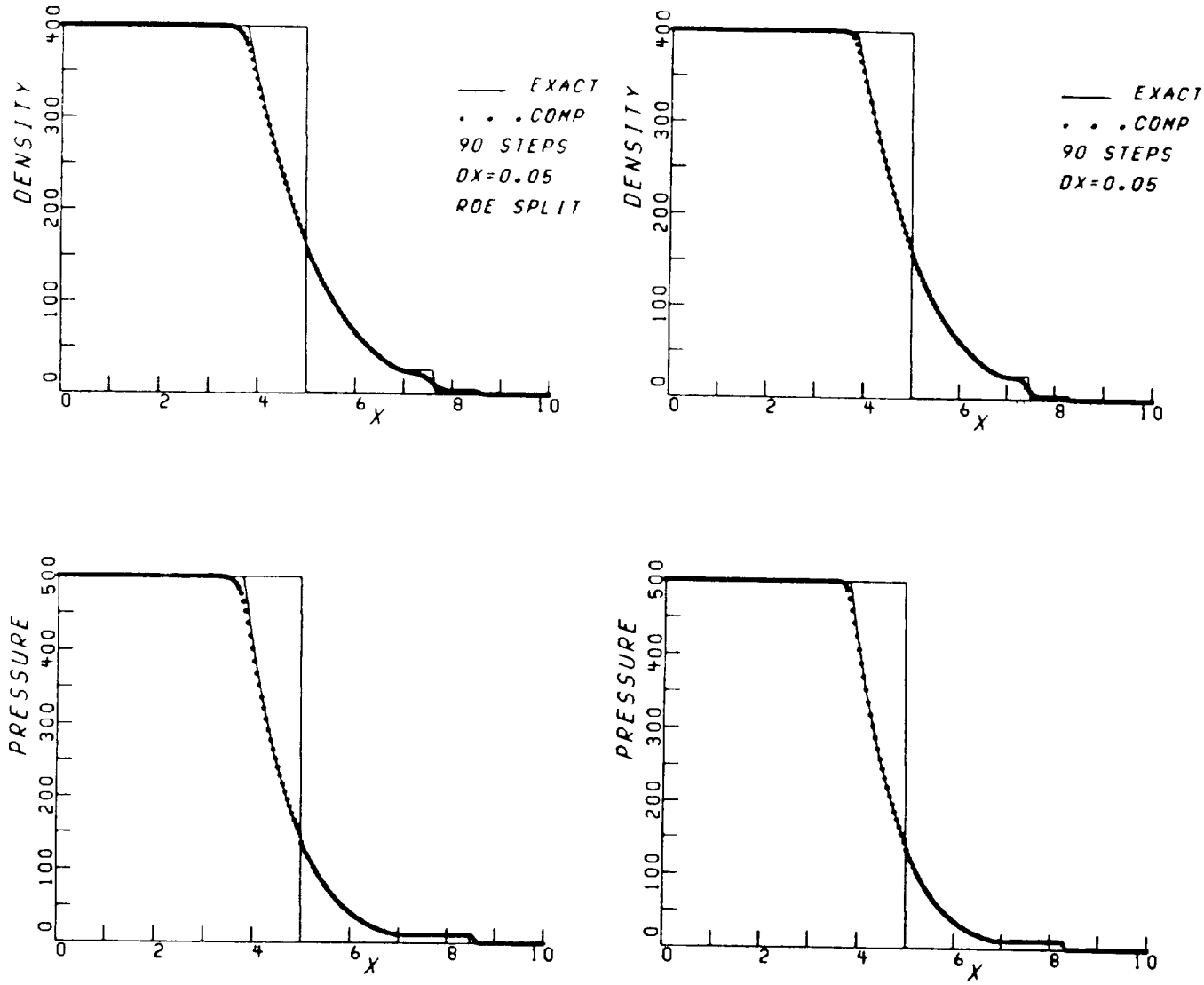


(a) TVD (b) ENO

Fig. 4. Numerical solutions of a strong shock problem

$$(\rho, u, p) = \begin{cases} (400, 0, 500), & x < 5 \\ (1, 0, 1), & x > 5 \end{cases}$$

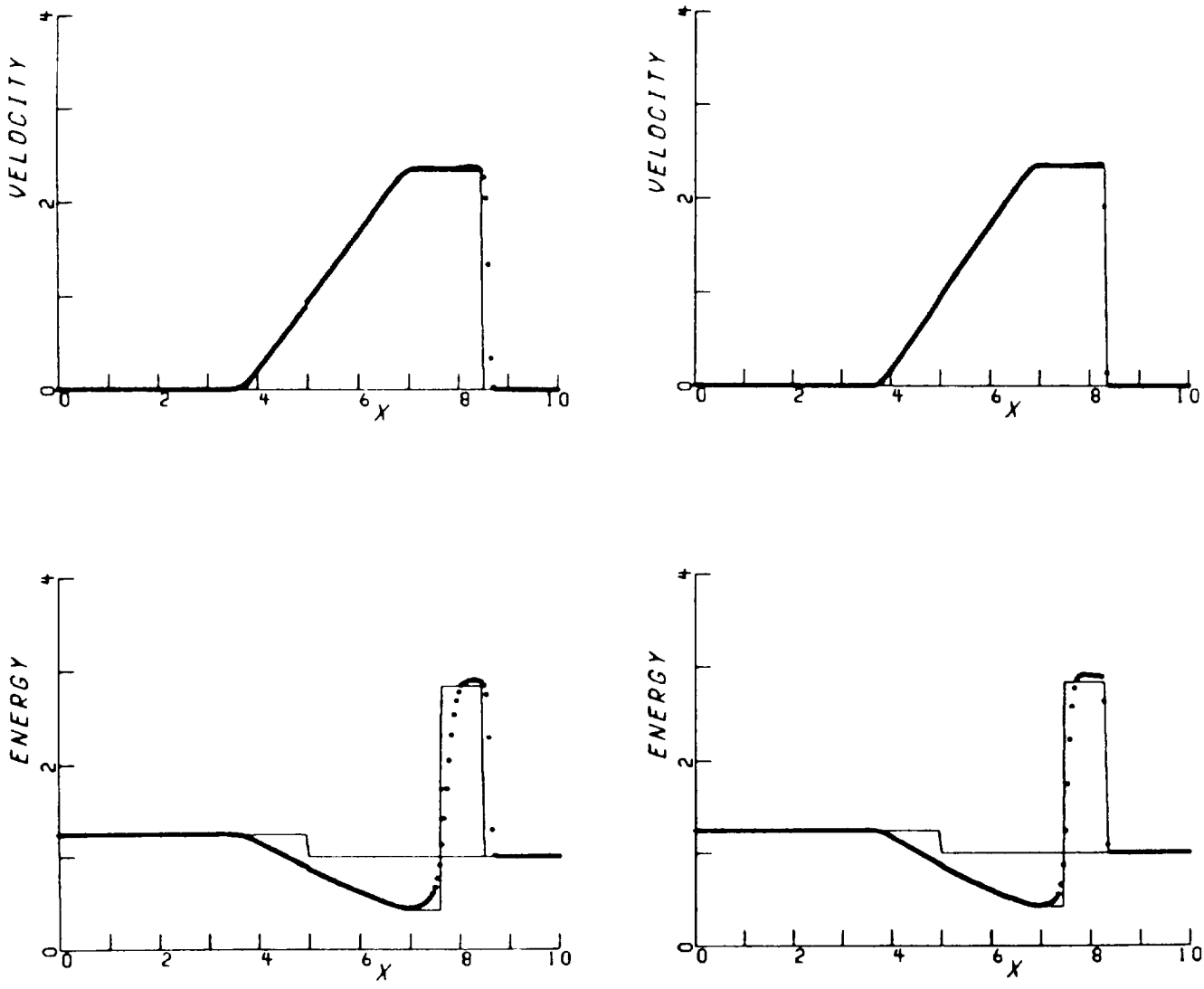


(a) TVD

(b) ENO

Fig. 4. Numerical solutions of a strong shock problem(continued)

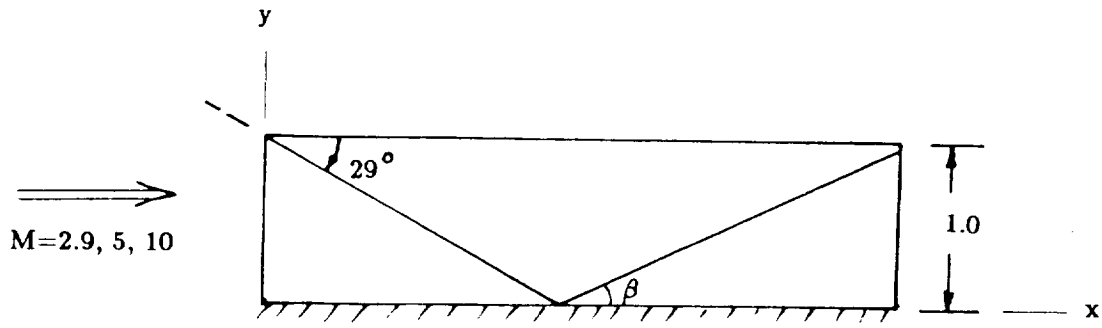


Fig. 5. Shock Reflection Problems
M=2.9, 5.0, 10.0; $\beta$=23.28, 16.99, 13.89 degrees respectively

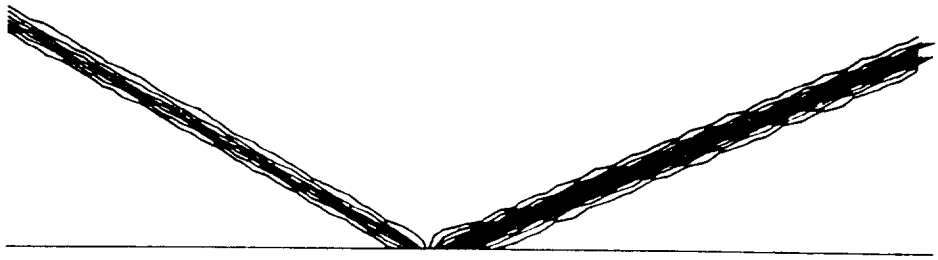

Fig. 6. Shock reflection problem, pressure contours from ENO computation
Mach number=2.9, shock angle=29 degrees

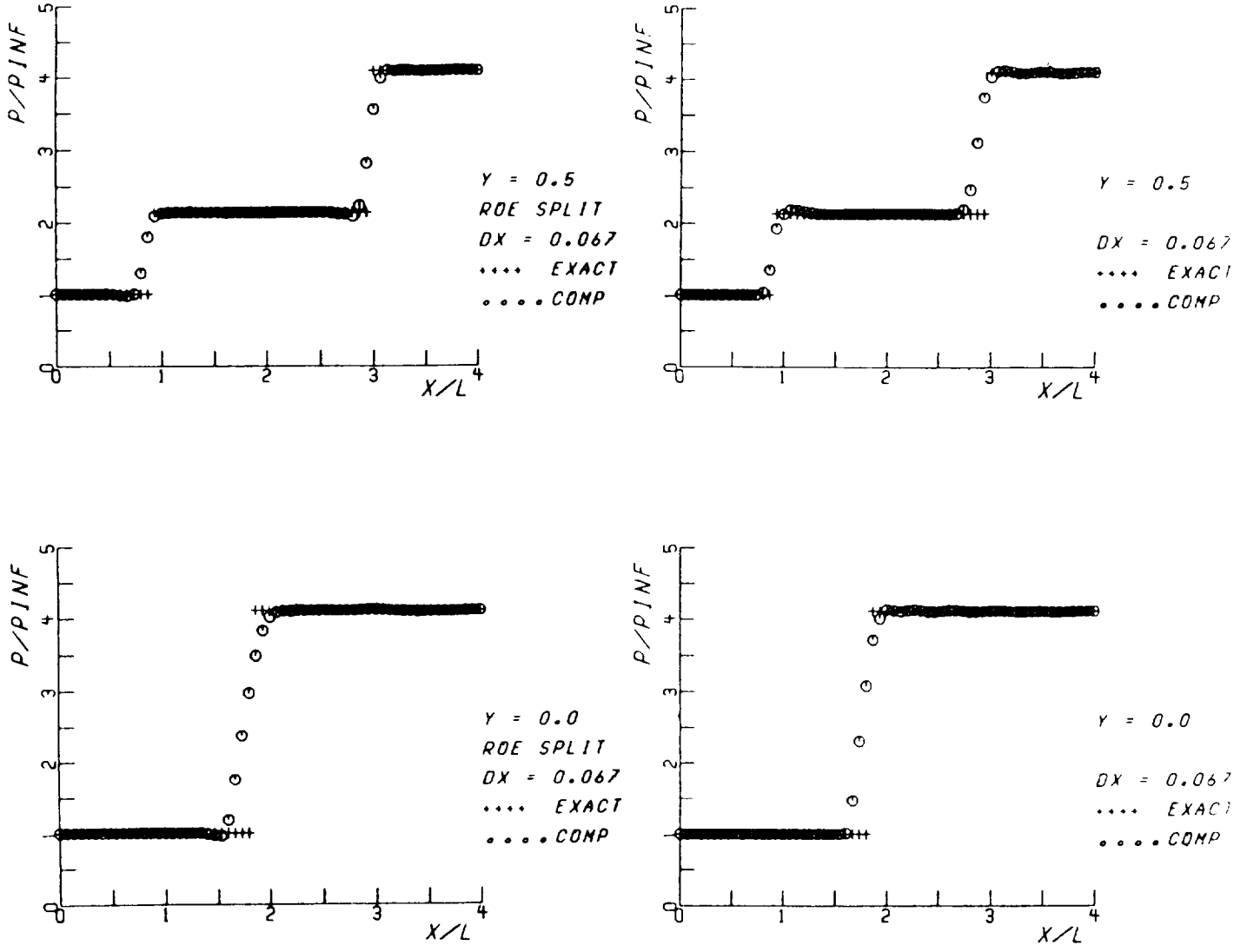


(a) TVD

(b) ENO

Fig. 7. Shock reflection problem, static pressure distribution at y=0 and y=0.5, Mach number=2.9, shock angle=29 degrees

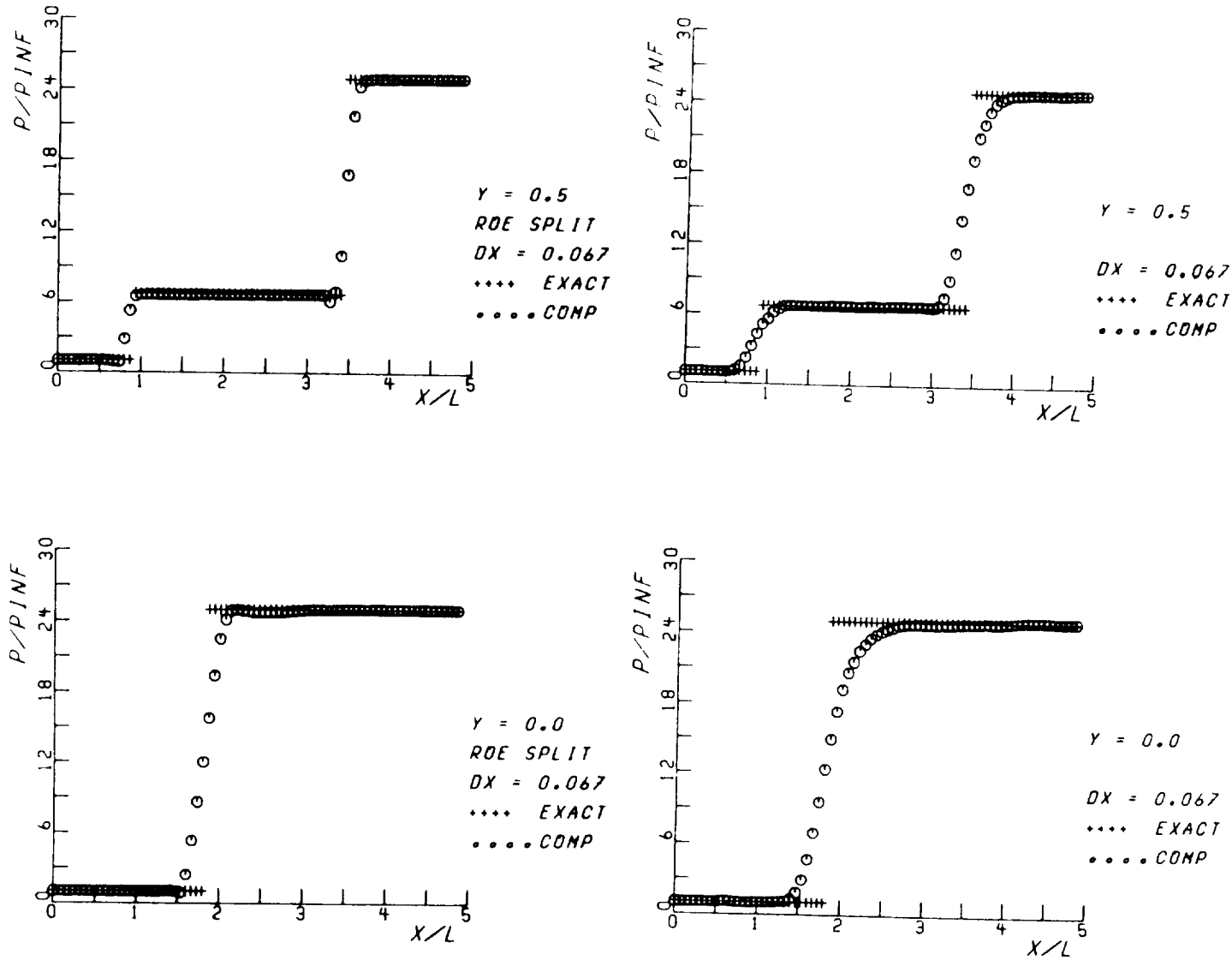


(a) TVD

(b) ENO

Fig. 8. Shock reflection problem, static pressure distribution at y=0 and y=0.5, Mach number=5.0, shock angle=29 degrees

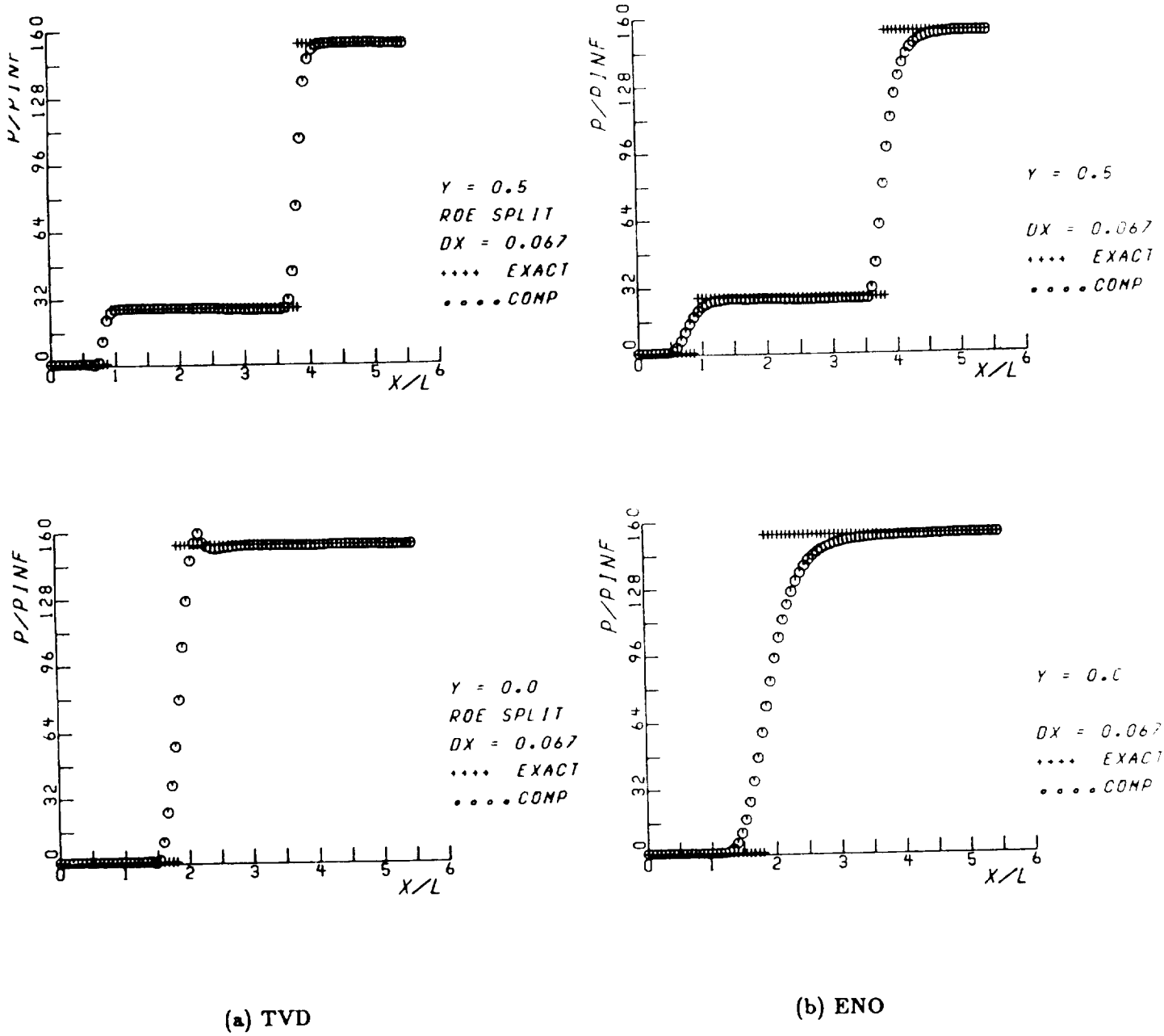


(a) TVD

(b) ENO

Fig. 9. Shock reflection problem, static pressure distribution at y=0 and y=0.5, Mach number=10.0, shock angle=29 degrees

NASA
National Aeronautics and Space Administration

# Report Documentation Page

| 1. Report No. | 2. Government Accession No. | 3. Recipient's Catalog No. |
|---|---|---|
| NASA TM-101355<br>ICOMP-88-18 | | |

| 4. Title and Subtitle | 5. Report Date |
|---|---|
| A Numerical Study of ENO and TVD Schemes for Shock Capturing | September 1988 |
| | 6. Performing Organization Code |

| 7. Author(s) | 8. Performing Organization Report No. |
|---|---|
| Shih-Hung Chang and Meng-Sing Liou | E-4384 |
| | 10. Work Unit No. |
| | 505-62-21 |

| 9. Performing Organization Name and Address | 11. Contract or Grant No. |
|---|---|
| National Aeronautics and Space Administration<br>Lewis Research Center<br>Cleveland, Ohio 44135-3191 | |
| | 13. Type of Report and Period Covered |
| | Technical Memorandum |

| 12. Sponsoring Agency Name and Address | 14. Sponsoring Agency Code |
|---|---|
| National Aeronautics and Space Administration<br>Washington, D.C. 20546-0001 | |

15. Supplementary Notes

Shih-Hung Chang, Department of Mathematics, Cleveland State University, Cleveland, Ohio 44115 and Institute for Computational Mechanics in Propulsion, NASA Lewis Research Center (work funded under Space Act Agreement C99066G); Meng-Sing Liou, NASA Lewis Research Center.

16. Abstract

The numerical performance of a second-order upwind-based TVD scheme and that of a uniform second-order ENO scheme for shock capturing are compared. The TVD scheme used in this study is a modified version of Liou, using the flux-difference splitting (FDS) of Roe and his "superbee" function as the limiter. The construction of the basic ENO scheme is based on Harten, Engquist, Osher, and Chakravarthy, and the 2D extensions are obtained by using a Strang-type of fractional-step time-splitting method. Numerical results presented include both steady and unsteady, 1D and 2D calculations. All the chosen test problems have exact solutions so that numerical performance can be measured by comparing the computed results to them. For 1D calculations, the standard shock-tube problems of Sod and Lax are chosen. A very strong shock-tube problems, with the initial density ratio of 400 to 1 and pressure ratio of 500 to 1, is also used to study the behavior of the two schemes. For 2D calculations, the shock wave reflection problems are adopted for testing. The cases presented in this report include flows with Mach numbers of 2.9, 5.0 and 10.0.

| 17. Key Words (Suggested by Author(s)) | 18. Distribution Statement |
|---|---|
| Shock capturing<br>ENO scheme<br>TVD scheme<br>Euler equations | Unclassified – Unlimited<br>Subject Category 64 |

| 19. Security Classif. (of this report) | 20. Security Classif. (of this page) | 21. No of pages | 22. Price* |
|---|---|---|---|
| Unclassified | Unclassified | 22 | A03 |

NASA FORM 1626 OCT 86

*For sale by the National Technical Information Service, Springfield, Virginia 22161